Cartilage-like composition of keloid scar extracellular matrix suggests fibroblast mis-differentiation in disease

Javier Barallobre-Barreiro[a], Elizabeth Woods[b], Rachel E. Bell[c], Jennifer A. Easton[c], Carl Hobbs[d], Michael Eager[b], Ferheen Baig[a], Alastair Mackenzie Ross[e], Raj Mallipeddi[f], Barry Powell[g], Mark Soldin[g], Manuel Mayr[a] and Tanya J. Shaw[c]

a - King's College London, *James Black Centre British Heart Foundation Centre, Denmark Hill Campus, London SE5 9NU, UK*
b - Division of Biomedical Sciences, *St George's University of London, London SW17 0RE, UK*
c - King's College London, *School of Immunology & Microbial Sciences, Department of Inflammation Biology, Centre for Inflammation Biology & Cancer Immunology, New Hunt's House, Guy's Campus, London SE1 1UL, UK*
d - King's College London, *Wolfson Centre for Age Related Diseases, Guy's Campus, London SE1 1UL, UK*
e - Guy's and St Thomas' NHS Foundation Trust, *Department of Plastic Surgery, Guy's Hospital, Great Maze Pond, London SE1 9RT, UK*
f - Guy's and St Thomas' NHS Foundation Trust, *St John's Institute of Dermatology, Cancer Centre, Great Maze Pond, London SE1 9RT, UK*
g - St George's University Hospitals NHS Trust, *Department of Plastic and Reconstructive Surgery, Blackshaw Road, London SW17 0QT, UK*

Correspondence to Tanya J. Shaw: *King's College London, Centre for Inflammation Biology & Cancer Immunology, New Hunt's House, Guy's Campus, London SE1 1UL, UK tanya.shaw@kcl.ac.uk.*
https://doi.org/10.1016/j.mbplus.2019.100016

Abstract

Following wound damage to the skin, the scarring spectrum is wide-ranging, from a manageable normal scar through to pathological keloids. The question remains whether these fibrotic lesions represent simply a quantitative extreme, or alternatively, whether they are qualitatively distinct. A three-way comparison of the extracellular matrix (ECM) composition of normal skin, normal scar and keloids was performed using quantitative discovery-based proteomics. This approach identified 40 proteins that were significantly altered in keloids compared to normal scars, and strikingly, 23 keloid-unique proteins. The major alterations in keloids, when functionally grouped, showed many changes in proteins involved in ECM assembly and fibrillogenesis, but also a keloid-associated loss of proteases, and a unique cartilage-like composition, which was also evident histologically. The presence of Aggrecan and Collagen II in keloids suggest greater plasticity and mis-differentiation of the constituent cells. This study characterises the ECM of both scar types to a depth previously underappreciated. This thorough molecular description of keloid lesions relative to normal scars is an essential step towards our understanding of this debilitating clinical problem, and how best to treat it.

Introduction

Scar formation, an inevitable consequence of the wound repair process, occurs with a range of severity. Mild cases may present only a minor aesthetic problem, but severe cases can drastically impede skin tissue functioning and be extremely debilitating. Keloid scars are an example of a pathological scar response which, in susceptible individuals, can develop from even a very minor insult (e.g. a vaccination injection)[1]. By definition, keloids are wound-induced skin lesions that expand beyond the original wound margin, often causing a tumour-like mass with excessive deposition of extracellular matrix (ECM) proteins. These lesions do not resolve with time and will frequently continue

growing for many years post-injury [1]. To date, there has been little clinical success in preventing or reducing normal or pathological skin scars, despite extensive testing of countless strategies [2]. This is attributed to our limited understanding of the mechanisms causing keloid disease, and how they contrast with the normal scar response.

Fibrosis is vaguely described as connective tissue deposition that can be excessive in pathological conditions. This suggests a quantitative spectrum of fibrosis wherein there can be more or less ECM, which in the context of a repairing skin wound could reflect the range from normal scar to keloid. This depiction, however, does not encompass the potential *qualitative* differences between normal and pathological scars. In keloids, the markedly different physical (hard and dense) and histological (hyalinization) characteristics compared to normal scars [3,4] indicate an altered and inappropriate matrix, rather than simply too much. A thorough molecular description of keloid lesions *relative to normal scars* is an essential step towards our understanding of this problem, and how best to treat it.

Gene expression profiling of normal skin versus keloids scars [5–7], and normal- versus keloid-derived fibroblasts [8] has provided insight into the mechanisms of scarring, but without a normal skin scar as a point of reference, it is still unknown which features are pathological. Nonetheless, these transcriptional analyses have identified important matrix and growth factor differences between normal skin and keloids, including many stereotypical scar-associated genes such as fibronectin (Fn) and TGFβ1, and interestingly a gene expression signature that includes typically cartilage-associated genes [e.g. cartilage oligomeric matrix protein (COMP)[8], and others [5]].

ECM composition is a balance of protein synthesis and degradation, and due to the slow turnover of many matrix proteins, it reflects an accumulation over time that necessitates protein analysis of tissue samples. Work in cardiovascular tissue has shown that quantitative proteomics allows for an unbiased strategy to discover the constituents of ECM and to compare between healthy and diseased tissue [9]. The pathological ECM associated with keloid disease has not been characterized in this manner or to this depth. This study investigates the differences in ECM composition between normal human skin (N), normal scar (S) and keloid (K) samples, which reveals misregulation of multiple functional categories of proteins that could contribute to keloidogenesis, and through identifying many keloid-unique components, indicates a qualitatively distinct lesion reminiscent of cartilage.

Results & discussion

In order to characterize and compare the ECM composition of keloids relative to normal skin and normal scars, skin samples were collected from 7 keloid patients and 5 melanoma re-excision patients (for paired normal skin-normal scar samples; patient/sample details in Supplementary Table S1). Following removal of the epithelium, dermis tissue was processed sequentially in NaCl buffer to extract loosely/ionically bound matrix proteins, SDS buffer to collect the cellular protein fraction (not analysed in this study), and Guanidine-HCl (GuHCl) buffer to extract integral matrix proteins. The NaCl and GuHCl proteins were deglycosylated and trypsin-digested in preparation for a discovery-based quantitative proteomic assessment (Supplementary Fig. S1)[10]. With this technique for tissue processing, 158 ECM proteins were detected in the NaCl extracts, and 108 in the GuHCl extracts (Supplementary Tables S2 and S3). The proteomic data has been deposited to the ProteomeXchange Consortium via the PRIDE partner repository with the dataset identifier PXD015057.

Qualitative differences in scar ECM composition

The proteomic data were first considered in a binary ("present or absent") manner in order to identify proteins unique to the different tissue types [threshold set at detection in ≥2 of 5/7 samples with ≥2 peptide-spectrum matches (PSM)]. This highlighted 13 ECM proteins only found in normal skin (interpreted as lacking in scars), 11 only found in normal scar, and strikingly, 23 keloid-unique ECM proteins, indicating that keloids are distinctive from normal scars (Fig. 1, Supplementary Table S4). The biological significance of these proteins is considered below, together with those that are not unique but quantitatively altered.

Quantitative differences in scar ECM composition

The paired nature of the normal skin-normal scar samples facilitated a robust quantitative comparison (Fig. 1B/D, heatmaps of differentially expressed proteins, *t*-test $p < 0.05$; Table 1) that served multiple purposes. First, this analysis revealed a level of complexity of the scar ECM that is generally underappreciated. Also, this pair-wise comparison validated the methodology in that many paradigm scar proteins were found to be significantly up-regulated [e.g. Tenascin (TNA), Periostin (POSTN), Fibronectin (FINC,FN), Thrombospondin (TSP) 1 & 2]. Finally, this provided the reference against which keloid composition was considered.

When normal scars were quantitatively compared to keloids, 21 proteins had significantly altered abundance in the NaCl extracts, and 9 in the GuHCl. Of note, the heatmap representations showed very clear delineation between the samples when considering the NaCl extracts (newly synthesized and/or loosely adherent proteins), but the differences were less clear

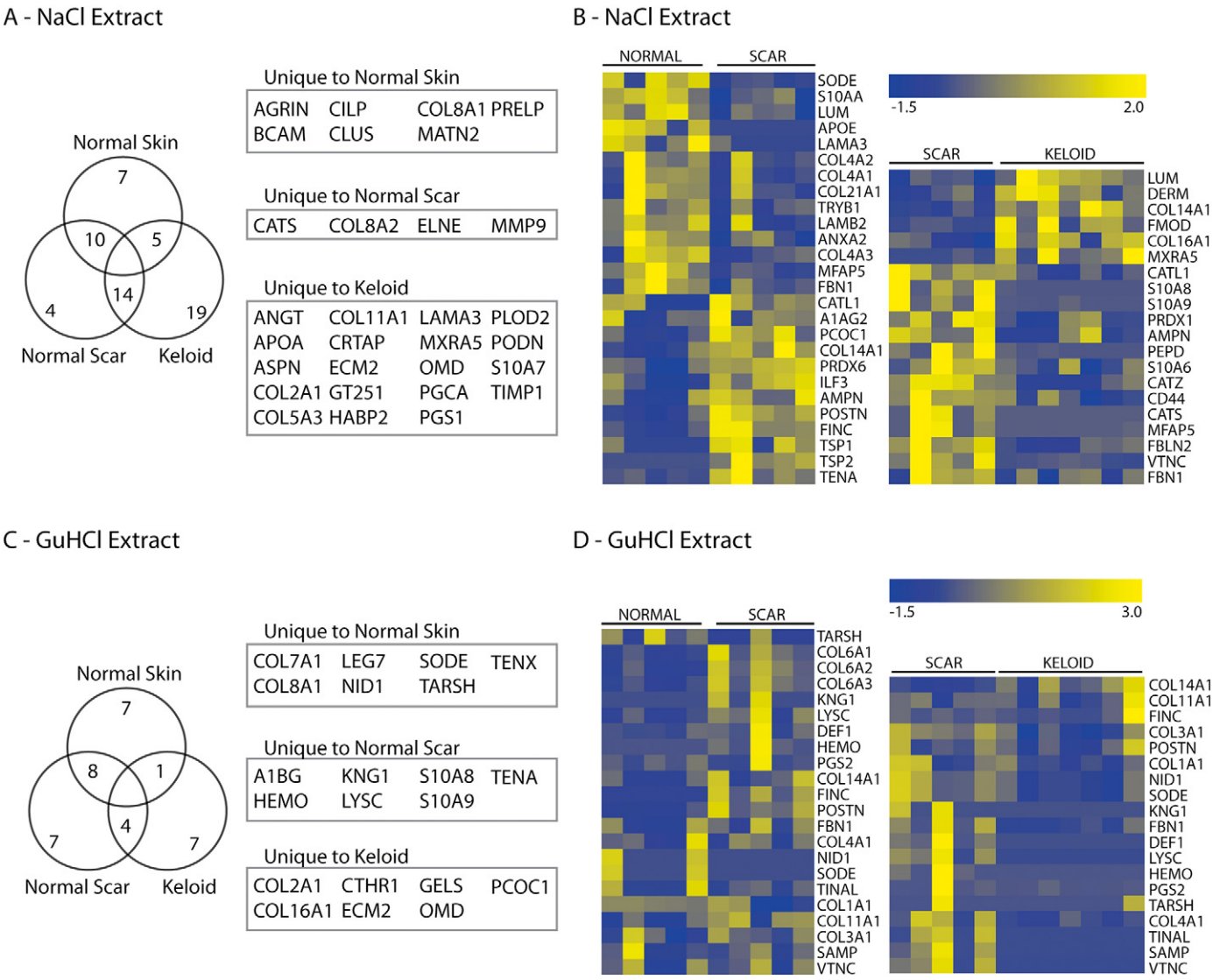

Fig. 1. Comparison of the ECM proteome (LC-MS/MS) of normal skin (n = 5), normal scars (n = 5) and keloid scars (n = 7). (A, C) Venn diagrams illustrating binary expression data in the three tissue types, with tissue-unique proteins listed (full lists in Supplementary Table S3). (B, D) Heatmaps of normalised abundances for proteins with significant differences ($p < 0.05$) for the comparisons shown. Proteins were clustered using hierarchical average linkage clustering using MeV software.

Table 1. ECM proteins with differential abundance between normal skin (N), normal scar (S), and/or keloid (K).

Abbrev	Full name	S/N fold change	p value (paired)	K/S fold change	p value (unpaired)	K/N fold change	p value (unpaired)	Extract
A1AG2	Alpha-1-acid glycoprotein 2	1.67	0.04	0.9	0.745	1.51	0.297	NaCl
AMPN	Aminopeptidase N	**2.67**	**0.002**	**0.34**	**0.048**	0.9	0.897	NaCl
ANXA2	Annexin A2	0.6	0.011	0.63	0.069	**0.38**	**0**	NaCl
APOE	Apolipoprotein E	**0.05**	**0.02**	40.77	0.379	2.23	0.624	NaCl
ASPN	Asporin	3.15	0.374	17.91	0.061	**56.48**	**0.049**	NaCl
PGBM	Basement membrane-specific heparan sulfate proteoglycan core protein	0.75	0.14	0.73	0.37	0.55	0.01	NaCl
COMP	Cartilage oligomeric matrix protein	25.79	0.179	12.28	0.067	**316.67**	**0.048**	NaCl
CATK	Cathepsin K	10.73	0.053	0.62	0.269	**6.62**	**0.021**	NaCl
CATS	Cathepsin S	8.34	0.112	**0.12**	**0.034**	1	n/a	NaCl
CATZ	Cathepsin Z	1.89	0.215	**0.2**	**0.002**	0.38	0.214	NaCl
CD44	CD44 antigen	1.4	0.13	**0.47**	**0.018**	0.66	0.245	NaCl
MUC18	Cell surface glycoprotein MUC18	0.61	0.277	0.24	0.087	**0.15**	**0.035**	NaCl
COL1A1	Collagen alpha-1(I) chain	0.92	0.192	0.9	0.113	**0.83**	**0**	GuHCl
COL3A1	Collagen alpha-1(III) chain	1.12	0.625	**0.61**	**0.021**	0.68	0.155	GuHCl
COL4A1	Collagen alpha-1(IV) chain	0.82	0.698	**0.14**	**0.015**	0.11	0.052	GuHCl
COL4A1	Collagen alpha-1(IV) chain	**0.43**	**0.007**	0.23	0.168	**0.1**	**0.005**	NaCl
COL7A1	Collagen alpha-1(VII) chain	0.42	0.186	0.64	0.439	**0.27**	**0.018**	NaCl
COL11A1	Collagen alpha-1(XI) chain	**3.22**	**0.035**	1.19	0.776	3.83	0.191	GuHCl
COL14A1	Collagen alpha-1(XIV) chain	**3.45**	**0.049**	**6.6**	**0.036**	**22.78**	**0.021**	GuHCl
COL14A1	Collagen alpha-1(XIV) chain	**2.24**	**0.032**	**2.88**	**0.011**	**6.45**	**0.002**	NaCl
COL16A1	Collagen alpha-1(XVI) chain	0.63	0.428	**3.16**	**0.012**	1.98	0.067	NaCl
COL18A1	Collagen alpha-1(XVIII) chain	0.88	0.801	0.29	0.112	**0.25**	**0.047**	NaCl
COL21A1	Collagen alpha-1(XXI) chain	**0.38**	**0.02**	0.29	0.25	**0.11**	**0.01**	NaCl
COL4A2	Collagen alpha-2(IV) chain	**0.48**	**0.006**	0.18	0.172	**0.09**	**0.021**	NaCl
PGS2	Decorin	1.67	0.638	0.18	0.263	**0.31**	**0.031**	GuHCl
DERM	Dermatopontin	2.67	0.074	**3.07**	**0.02**	**8.21**	**0.003**	NaCl
SODE	Extracellular superoxide dismutase	**0.23**	**0.026**	1.89	0.363	0.44	0.07	NaCl
SODE	Extracellular superoxide dismutase	0	0.178	undef	n/a	0	0.077	GuHCl
FBN1	Fibrillin-1	0.54	0.044	0.53	0.048	**0.29**	**0.002**	NaCl
FBN1	Fibrillin-1	1.55	0.499	**0.12**	**0.022**	0.19	0.15	GuHCl
FMOD	Fibromodulin	0.15	0.36	**12.54**	**0.042**	1.87	0.393	NaCl
FINC	Fibronectin	**4.35**	**0.019**	0.84	0.663	3.66	0.077	NaCl
FINC	Fibronectin	>**1000**	**0.029**	1.94	0.624	>1000	0.318	GuHCl
FBLN2	Fibulin-2	0.83	0.414	**0.24**	**0.002**	**0.2**	**0.022**	NaCl
LEG3	Galectin-3	0.92	0.722	0.71	0.151	0.66	0.03	NaCl
LEG7	Galectin-7	0.25	0.095	0.39	0.229	**0.1**	**0.021**	NaCl
ILF3	Interleukin enhancer-binding factor 3	**3.5**	**0.034**	0.83	0.53	2.9	0.073	NaCl
LAMA3	Laminin subunit alpha-3	**0.1**	**0.039**	2.58	0.371	**0.25**	**0.031**	NaCl
LAMA5	Laminin subunit alpha-5	0.53	0.099	0.46	0.461	**0.24**	**0.034**	NaCl
LAMB2	Laminin subunit beta-2	**0.42**	**0.042**	0.55	0.497	**0.23**	**0.003**	NaCl
LAMC1	Laminin subunit gamma-1	0.64	0.073	0.58	0.238	**0.37**	**0.019**	NaCl
LUM	Lumican	**0.45**	**0.026**	**2.61**	**0.008**	1.17	0.478	NaCl
LYSC	Lysozyme C	6.31	0.119	**0**	**0.011**	0	0.097	GuHCl
MXRA5	Matrix-remodeling-associated protein 5	1.03	0.374	**19.77**	**0.044**	**20.37**	**0.035**	NaCl
MFAP5	Microfibrillar-associated protein 5	**0.13**	**0.022**	**0.03**	**0.044**	**0**	**0.001**	NaCl
DEF1	Neutrophil defensin 1	3.1	0.301	0	0.056	**0**	**0.005**	GuHCl
NID1	Nidogen-1	0.52	0.309	0.52	0.484	**0.27**	**0.012**	NaCl
NID1	Nidogen-1	0	0.179	**0.9**	**0.016**	**0**	**0.078**	GuHCl
OMD	Osteomodulin	8.84	0.351	3.53	0.129	**31.19**	**0.023**	NaCl
POSTN	Periostin	**4.64**	**0.007**	0.95	0.886	4.39	0.061	NaCl
POSTN	Periostin	**11.24**	**0.034**	0.74	0.556	8.3	0.1	GuHCl
PRDX1	Peroxiredoxin-1	1.27	0.423	0.62	0.014	0.78	0.369	NaCl
PRDX6	Peroxiredoxin-6	1.96	0.021	0.67	0.175	1.31	0.536	NaCl
PCOC1	Procollagen C-endopeptidase enhancer 1	**3.32**	**0.031**	**2.41**	**0.05**	**8**	**0.007**	NaCl
AMBP	Protein AMBP	0.70	0.26	**0.46**	**0.02**	**0.32**	**0**	NaCl
S10AA	Protein S100-A10	**0.45**	**0.002**	0.52	0.087	**0.23**	**0**	NaCl
S10A6	Protein S100-A6	1.17	0.722	0.66	0.043	0.78	0.547	NaCl
S10A8	Protein S100-A8	6.33	0.088	**0.01**	**0.009**	**0.07**	**0.003**	NaCl
S10A9	Protein S100-A9	12.33	0.076	**0.04**	**0.017**	0.45	0.339	NaCl
SAMP	Serum amyloid P-component	0.39	0.068	0.06	0.096	**0.02**	**0.031**	NaCl
SAMP	Serum amyloid P-component	0.76	0.786	**0**	**0.018**	0	0.141	GuHCl
TARSH	Target of Nesh-SH3	**0.31**	**0.04**	0.43	0.569	**0.13**	**0.047**	GuHCl
TENA	Tenascin	**8.67**	**0.049**	0.34	0.076	2.91	0.182	NaCl
TSP1	Thrombospondin-1	**8.08**	**0.032**	0.84	0.675	**6.8**	**0.036**	NaCl
TSP2	Thrombospondin-2	**20.76**	**0.043**	1.38	0.595	28.6	0.053	NaCl
TRYB1	Tryptase alpha/beta-1	**0.45**	**0.038**	1.23	0.568	0.55	0.127	NaCl

Table 1 (*continued*)

Abbrev	Full name	S/N fold change	p value (paired)	K/S fold change	p value (unpaired)	K/N fold change	p value (unpaired)	Extract
TINAL	Tubulointerstitial nephritis antigen-like	0.39	0.403	**0**	**0.016**	0	0.083	GuHCl
VTNC	Vitronectin	0.52	0.089	**0.09**	**0.005**	**0.05**	**0.004**	NaCl
VTNC	Vitronectin	1.04	0.951	**0**	**0.008**	**0**	**0.027**	GuHCl
PEPD	Xaa-Pro dipeptidase	1.65	0.394	**0.05**	**0.016**	**0.08**	**0.048**	NaCl

Undef: Undefined (to describe the ratio when protein was considered undetected); in these cases, p value was assigned n/a.
Bold values highlight proteins with >2-fold or < 0.5-fold change.

in the GuHCl extract (enriched for integral, cross-linked components). This implies that even keloids that are many years old at time of excision are still actively synthesizing new ECM, and this also may indicate that the most significant distinguishing features of the two scar types are within the newly synthesized fraction. Also noteworthy was that keloids, compared to normal scars, had more proteins significantly down-regulated than up-regulated.

Altered fibrillogenesis and ECM assembly

The major alterations in keloid composition relative to normal scars, when functionally grouped, showed many changes in proteins involved in ECM assembly and fibrillogenesis. This was perhaps expected based on the variable histological appearance, in particular when stains such as Haematoxylin Van Gieson (HVG) are used to selectively colour collagens (Fig. 2A). Amongst the unique and most significantly altered in the pathological context were FACIT collagens (fibrillar associated collagens with interrupted triple helices) Collagens XII, XIV, and XVI (COL12A1, COL14A1, COL16A1; Fig. 2B). This family has the potential to alter the organization and stability of the most abundant and more commonly discussed fibrillar collagens including Collagens I and III [11] and thus may be implicated in scarring and fibrosis [12–14]. Another family of proteins involved in fibril assembly, organization and degradation (amongst other important immunological functions, but relatively unexplored influence on skin scarring) are the small leucine rich proteoglycans (SLRPs)[15]. Asporin, Biglycan, ECM2 and Osteomodulin are four such proteins identified to be unique to keloid matrix (Fig. 2C). Asporin was similarly identified to be over-represented in keloid scars by Ong et al [16], in their comparison of non-decellularised keloid tissue to normal skin using 2D gel electrophoresis followed by mass spectrometry to identify the differentially expressed proteins. Indeed, the family of proteins has an increasing reputation for functionally contributing to fibrotic responses in various organ systems [17].

Collagens I and III and the ratio between the two are industry standards for scar research, although the data are surprisingly conflicting [18–20]. Nonetheless, Collagen I is frequently described to accumulate in fibrotic lesions and is more highly transcribed by scar fibroblasts relative to healthy or non-healing tissue or cells [21]. Also, the dynamics of the Collagen I/Collagen III ratio is acknowledged to first decrease in granulation tissue during wound healing, due to the transient increase in Collagen III; the ratio then returns to normal [22], or equilibrates with elevated I/III ratio [20]. Here, our comparison of normal scars to normal skin (focussing on the GuHCl extracts) demonstrated that normal scars had a lower Collagen I/Collagen III ratio suggesting a lack of maturity [calculated using the abundance of COL1A1÷2 (Collagen I trimer is 2× COL1A1 chains plus 1× COL2A1 chain) divided by COL3A1÷3 (Collagen III trimer is 3× COL3A1 chains)]. Of interest, the keloids had less of both COL1A1 and COL3A1, and a high variability in I/III ratio across patients (Supplementary Fig. S2). Although in conflict with transcriptional data, this result may truly reflect lower protein abundance in the extracellular space due, for example, to a shortcoming in its assembly. Alternatively, this could reflect a greater insolubility of the fibrillar collagens in keloids, perhaps due to higher cross-linking mechanisms, and in turn a failure to extract them. Nonetheless, the fibrillar collagen network is *different* in disease.

Fibronectin (FN) is also a fibrillar ECM protein whose transcriptional up-regulation is a gold-standard biomarker of fibrosis [21,23]. In our tissue samples, FN protein showed the anticipated and significant increase in normal scars relative to normal skin, but in keloids levels were highly variable and importantly not more abundant than in normal scars (Supplementary Fig. S2). The binary distribution of FN expression was striking, suggesting that there may be single nucleotide polymorphisms or mutations in pathways regulating its expression that distinguish the patients with high vs low levels of this protein (e.g. TGFβ1 pathway [24], *NEDD4* [25]). The patient samples included in this study were randomly selected and unfortunately, we do not know about genetic mutations that may be present.

Vitronectin is another protein associated with fibrillar extracellular matrix that was identified to be altered in keloids; specifically, it was notably under-represented with <10% the amount of normal skin

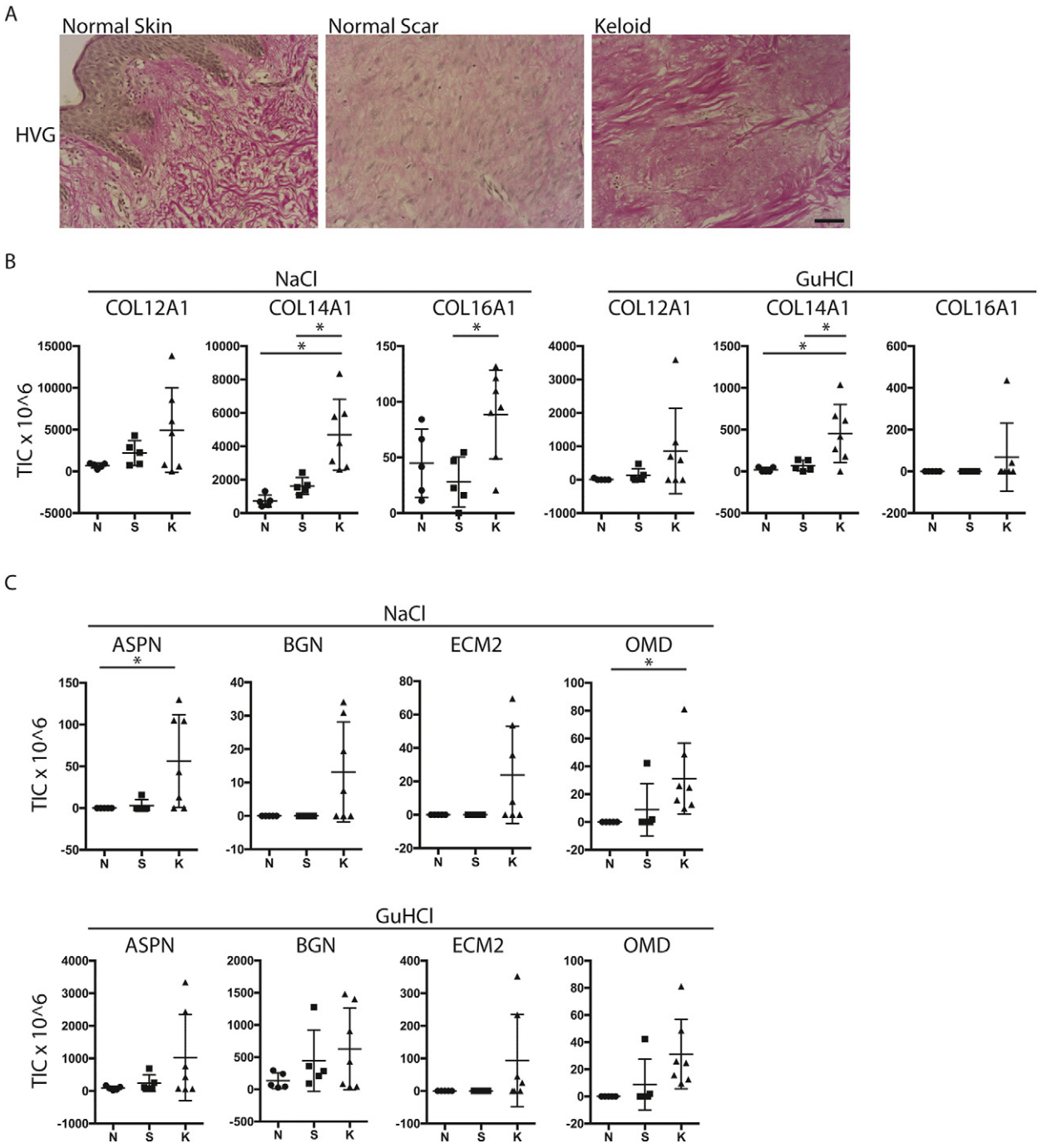

Fig. 2. Alterations in collagen organization in keloid scar. (A) Histological sections stained with Haematoxylin Van Gieson (HVG). Scale bar: 50 µm. (B, C) Abundance (Total Ion Current, TIC) of (B) FACIT collagens and (C) SLRPs in NaCl and GuHCl extracts of normal skin (N, n = 5), normal scar (S, n = 5), and keloid (K, n = 7). Results are graphed as mean ± SD, with individual values shown. Statistical significance was calculated using Students *t*-test (*, $p < 0.05$).

and normal scar. This was unexpected in light of the reports of elevated expression in fibrotic liver [26] and lung [27], but its absence may highlight interestingly divergent cellular mechanisms leading to different scar conditions.

Scar-associated reduction in basement membrane proteins

One functional category of ECM proteins significantly down-regulated in normal scars relative to

normal skin, and further down again in keloids, were those associated with the basement membrane [28]. Specifically, COL4A1, COL7A1, and Laminin A3 (LAMA3) were all less abundant in scars and keloids (Supplementary Fig. S3). However, immunohistochemistry (IHC) of Collagen IV grossly showed an intact basement membrane between the epidermis and dermis in all tissue types, although ultrastructurally and functionally there may be differences that were not apparent with this approach [29]. Instead, the dramatically reduced levels of the BM proteins in scars and keloids are alternatively thought to reflect fewer undulations in the epidermal-dermal boundary, and also fewer blood vessels (Supplementary Fig. S3). There are varying reports on blood vessel density in keloids [30,31] potentially due to the location within the lesion under analysis, but keloids are consistently recognized to be hypoxic, a feature which is thought to functionally contribute to their development [32].

Reduced proteases in pathological scars

Comparing normal, ultimately resolving scars with keloids revealed numerous proteases with relevant extracellular substrates to be lacking in the pathological context. Specifically, Cathepsins S and Z were less abundant in keloids, as were AMPN (Aminopeptidase N) and PEPD (Prolidase) (Supplementary Fig. S4). Although there are no reports about Cathepsin Z in fibrotic disease, Cathepsin S expression and function has been positively associated with fibrosis before, with high expression associated with poorer outcomes in idiopathic pulmonary fibrosis [33]. Perhaps its elevated expression in fibrotic lung, as with the normal scars in our study, yet its absence in keloids, reflect the age/maturity of the fibrotic lesions, and/or variations in cell populations responsible for producing the enzyme. Regardless, an imbalance between proteases and their inhibitors is clearly important in the development of fibrotic diseases [34]. The cathepsin family of proteases specifically, whether over-abundant as in lung fibrosis, or under-abundant as in keloids, represent interesting candidates to have important functional roles in scarring, because of their potential to modulate not only the ECM (Supplementary Fig. S4)[35], but also immune cell activation [36] and fibrosis-relevant signalling pathways [37].

A unique cartilage-like composition in keloids

Most strikingly, a cartilage-like composition was found in keloids, distinguishing them from the other two tissue types. When all of the proteins that are keloid-unique and/or quantitatively up-regulated relative to normal scars were considered together (27 proteins), 17 can have functions in cartilage development or homeostasis (Fig. 3A). The data for aggrecan (PGCA), the archetypal cartilage proteoglycan, is shown, illustrating marked upregulation in keloids in the NaCl extract and unique detection in the GuHCl protein fraction (Fig. 3B). Consistent with this, histological (H&E) analysis of the hyalinised regions of keloids (a defining histological feature) emphasized a matrix uniformity reminiscent of cartilage (Fig. 3C). We also compared keloid histology to both normal skin and normal scar using Alcian Blue, pH 2.5 for acidic polysaccharides such as glycosaminoglycans characteristic of cartilage. Batch staining of 28 keloid cases, 9 normal skin samples and 4 normal scars followed by quantitative assessment of the number of pixels exceeding a threshold intensity showed significantly enhanced staining in the keloid samples. The keloid sample uptake of alcian blue stain was significantly higher, however, there was notable heterogeneity and also mild staining in the normal scar compared to normal skin (Fig. 3C, D).

We consider the cartilage-like features to distinguish keloids from normal scars of the skin, but in fact there may be other pathological fibrotic conditions that share these attributes. For example, studies of fibrotic heart and liver both identified extracellular aggrecan protein to be significantly elevated [9,38], cartilage oligomeric matrix protein (COMP) has been detected in other examples of pathological skin fibrosis (e.g. scleroderma) [39], and likely there are similar mechanisms at work in vascular changes in disease [40].

Our observations hint at a chondrocyte-like phenotype for the constituent cells. The chondrogenic potential of dermal fibroblasts has been explored extensively for regenerative medicine purposes, which has realized that autologous dermal fibroblasts are relatively easily manipulable into chondrocytes [41]. Ominously, this can be partly achieved with growth factors and signalling molecules abundant in a wound milieu [42]. The unique cartilage-like profile of the keloids could also support a hypothesis that the precursor cell of these pathological scars is particularly plastic [43]. Defining the initiating cell is difficult in the absence of an animal model and an ability to lineage-trace [44], but emerging technologies may help answer this important question in the future.

Certainly, the transcriptional profile of keloid-derived fibroblasts has previously been reported to contain important chondrocytic genes [5,8]. To begin to understand whether the key proteins identified here may be regulated transcriptionally, we analysed existing microarray datasets on keloid tissue (Gene Expression Omnibus Accession numbers GSE90051 [45] and GSE92566 [46]). This identified that 20 of the 27 keloid-associated proteins (unique or quantitatively increased) are similarly over-abundant at the transcriptional level (Supplementary Table S5). Signalling

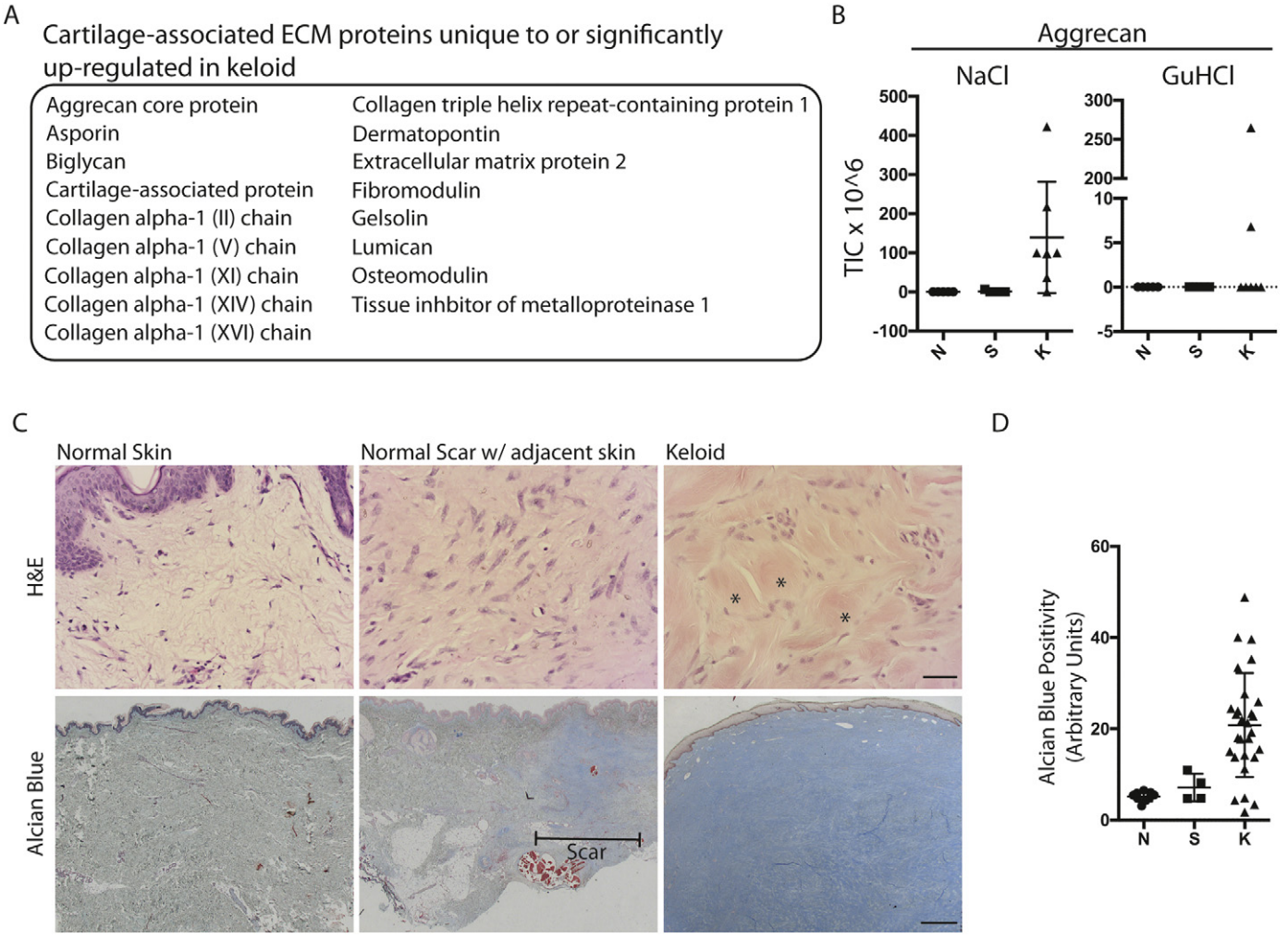

Fig. 3. Cartilage-like composition in keloid scars. (A) A list of the 17 of 27 keloid-associated proteins implicated in cartilage development or homeostasis. (B) Abundance (Total Ion Current, TIC) of Aggrecan in NaCl and GuHCl extracts of normal skin (N, n = 5), normal scar (S, n = 5), and keloid (K, n = 7). Results are graphed as mean ± SD, with individual values shown. (C) Histological sections stained with Haematoxylin and Eosin (H&E; scale bar: 50 μm; * indicate areas of hyalinisation) or Alcian Blue, pH 2.5 (scale bar: 200 μm). (D) Quantitative assessment of the number of pixels exceeding a threshold intensity of blue, following batch staining of the tissues. Results are graphed as mean ± SD, with individual values shown.

pathways and key transcription factors regulating chondrocyte differentiation are well described [42,47], and we suggest these may represent appropriate therapeutic targets. Targeting this mis-differentiation may present an opportunity to stop keloid development at the root cause, halting development of the culpable cell type. This should in turn ameliorate the hard and stiff physical attributes of keloids, which are thought to contribute to the pain associated with the lesions, and also the impermeability of injected treatments.

This study employed a discovery-based proteomic strategy to improve the characterisation of keloid scars relative to non-pathological lesions. We have found that keloids have a distinct ECM composition, which in some respects are reminiscent of cartilage. These observations provide important insight into the molecular mechanisms underlying disease and potential therapeutic targets for future investigation.

Experimental procedures

Tissue collection and processing

This work was ethically approved by the National Research Ethics Service (UK) and institutionally sponsored (St George's, University of London). All subjects provided informed consent and the study was conducted in accordance with the ethical standards as set out in the WMA Declaration of Helsinki and the Department of Health and Human Services Belmont Report. Briefly (additional information available in the Supplementary Material), surplus skin tissue was obtained from patients undergoing reductive plastic surgery, normal scars were from melanoma re-excision patients, and keloid scars from revision procedures (sample details in Supplementary Table S1). For histology and immunohistochemistry, samples were promptly fixed in 4% paraformaldehyde and embedded in paraffin according to standard protocols. Samples for protein extraction were trimmed of subcutaneous fat and washed sequentially in iodine (2.5 mg/ml), 70% ethanol, and gentamycin solution (final concentration 0.5 mg/ml, Sigma), and incubated in Dispase II (1 U/ml in Hanks Balanced Salt Solution, Sigma) overnight at 4 °C to remove the epidermis. Next, the dermis was snap frozen in liquid nitrogen for future protein extraction.

Extraction and preparation of extracellular space proteins

All solutions for protein extraction contained commercially available protease and phosphatase inhibitor cocktails (Sigma-Aldrich) and 25 mM EDTA to ensure inhibition of metalloproteinases. 50–100 mg of tissue per sample were diced, rinsed in ice-cold phosphate buffered saline (PBS) to remove plasma contaminants, then incubated with 10:1 volume (i.e. 1 ml for 100 mg) 0.5 M NaCl, 10 mM Tris pH 7.5 with mild vortexing for 2 h at room temperature. Next, the cellular protein fraction was collected by incubating the tissue in 0.08% SDS for 4 h with vortexing. Finally, the samples were incubated in 4 M GuHCl (+ 50 mM sodium acetate pH 5.8; 5:1 volume:weight ratio) 48 h at room temperature. Next, zirconium beads were added to the samples and the tubes were vortexed vigorously to enhance mechanical disruption. GuHCl and NaCl extracts were precipitated with ethanol, pelleted, then dried and re-dissolved in deglycosylation buffer. (Supplementary Fig. S1; additional methodology details available in Supplementary Material).

A previously published, two-step deglycosylation protocol was pursued to ensure pan-deglycosylation [10,48]. Next, deglycosylated NaCl/GuHCl extracts were denatured using a final concentration of 6 M urea, 2 M thiourea and reduced by the addition of DTT (final concentration 10 mM) followed by incubation at 37 °C for 1 h, 240 rpm. The samples were then alkylated by the addition of 0.5 M iodoacetamide (final conc. 50 mM), and finally precipitated with acetone. Protein pellets were dried using a speedvac, re-suspended in 0.1 M TEAB buffer, pH 8.2, containing trypsin (1:50 trypsin:protein), and digested. The digest was stopped by acidification of the samples with 10% trifluoroacetic acid (TFA; final concentration 1% TFA). Peptide samples were purified using a 96-well C18 spin plate. The eluates were frozen at −80 °C for 2 h before being lyophilized (Sciquip, Alpha 1–2 LD plus) at −55 °C overnight.

Liquid chromatography and tandem mass spectrometry analysis (LC-MS/MS)

The lyophilised peptide samples were reconstituted with 0.05% TFA in 2% ACN and separated on a nanoflow LC system (Dionex UltiMate 3000 RSLCnano). Samples were injected onto a nano-trap column (Acclaim® PepMap100 C18 Trap, 5mm×300µm, 5 µm, 100 Å), at a flow rate of 25 µL/min for 3 mins, using 2% ACN, 0.1% formic acid (FA) in H_2O. The nano LC gradient used to separate the peptides at 0.3 µL/min is described in the Supplementary Material. The nano column (Acclaim® PepMap100 C18, 50cmx75µm, 3 µm, 100 Å) was set at 40 °C and coupled to a nanospray source (Picoview, New Objective, US). Spectra were collected from a Q Exactive Plus (Thermo Fisher Scientific) using full MS mode (resolution of 70,000 at 200 *m/z*) over the mass-to-charge (m/z) range 350–1600. Data-dependent MS2 scan was performed using the top 15 ions in each full MS scan (resolution of 17,500 at 200 m/z) with dynamic exclusion enabled. Thermo Scientific Proteome Discoverer software (version 1.4.1.14) was used

to search raw data files against the human database (UniProtKB/Swiss,Prot version 2016_02, 20,198 protein entries) using Mascot (version 2.3.01, Matrix Science). Scaffold (version 4.1.1, Proteome Software Inc., Portland, OR) was used to validate MS/MS-based peptide and protein identifications with the following filters: a peptide probability of >95.0% (as specified by the Peptide Prophet algorithm), a protein probability of >99.0%, and at least two independent peptides per protein. Files were converted for submission to PRIDE using Scaffold (version 4.7.3). The proteomic data has been deposited to the ProteomeXchange Consortium via the PRIDE partner repository with the data set identifier PXD015057.

Western blotting

Protein extracted for proteomics as described above (5 μg) was also subjected to SDS-PAGE and western blotting using the Invitrogen NuPAGE system as recommended by the manufacturer (Life Technologies). The PVDF membrane was first stained with Ponceau S for total protein, then blotted for Fibronectin (Abcam antibody ab23750; additional details in Supplementary Material).

Histology and Immunohistochemistry (IHC)

FFPE tissue was sectioned at 7–10 μm and batch-stained with haematoxylin and eosin (H&E), Alcian Blue (pH 2.5), or Haematoxylin Van Gieson (HVG) according to standard protocols. Alcian Blue uptake was quantified using Image J (NIH). Immunohistochemistry for Collagen IV expression was carried out on FFPE tissue according to antibody manufacturers' instructions (see Supplementary Material).

Statistics

For quantification of proteins by mass spectrometry, the adjusted total ion current (TIC) was used. Comparisons of protein abundance were achieved using Students *t*-tests (paired, N vs S; unpaired, S vs K and N vs K). MultiExperiment Viewer software (MeV, TM4) was used to facilitate visualization. TIC values were transformed to N(0,1). Significance was inferred for p-values of <0.05 for all tests (not adjusted for multiple comparisons). When proteomics data are graphed, mean ± SD are shown.

Supplementary data to this article can be found online at https://doi.org/10.1016/j.mbplus.2019.100016.

Author contributions

JBB: methodology, validation, formal analysis, investigation, data curation, writing – review & editing, visualization; EW: formal analysis, investigation, writing – review & editing, visualization; REB: investigation, resources, writing – review & editing; JE: investigation, resources, writing – review & editing; CH: investigation; ME: investigation, formal analysis, visualization; FB: methodology, validation, data curation, writing – review & editing; AMR: resources; RM: resources; BP: resources; MS: resources, writing – review & editing; MM: conceptualization, methodology, resources, data curation; TS: conceptualization, validation, investigation, resources, data curation, writing – original draft, writing – review & editing, visualization, project administration, funding acquisition.

Declaration of competing interest

The authors have declared that no conflict of interest exists.

Acknowledgements

TS acknowledges the Medical Research Council and the British Skin Foundation for funding. JBB is a Career Establishment Fellow in the King's British Heart Foundation Centre. MM is a Senior Fellow of the British Heart Foundation. The study was supported by the NIHR Biomedical Research Centre based at Guy's and St. Thomas' National Health Service Foundation Trust and King's College London in partnership with King's College Hospital.

Received 23 August 2019;
Received in revised form 16 September 2019;
Accepted 16 September 2019
Available online 30 October 2019

Keywords:
Wound;
Differentiation;
Plasticity;
ECM;
Scar;
Fibrosis

References

[1] J.P. Andrews, J. Marttala, E. Macarak, J. Rosenbloom, J. Uitto, Keloids: the paradigm of skin fibrosis - pathomechanisms and treatment, Matrix Biol. 51 (2016) 37–46.

[2] T. J. Shaw, K. Kishi, R. Mori, Wound-associated skin fibrosis: mechanisms and treatments based on modulating the inflammatory response, Endocr Metab Immune Disord Drug Targets 10 (4) (2010) 320–330.
[3] J.Y. Lee, C.C. Yang, S.C. Chao, T.W. Wong, Histopathological differential diagnosis of keloid and hypertrophic scar, Am. J. Dermatopathol. 26 (5) (2004) 379–384.
[4] N. Jumper, R. Paus, A. Bayat, Functional histopathology of keloid disease, Histol. Histopathol. 30 (9) (2015) 1033–1057.
[5] M. Naitoh, H. Kubota, M. Ikeda, T. Tanaka, H. Shirane, S. Suzuki, K. Nagata, Gene expression in human keloids is altered from dermal to chondrocytic and osteogenic lineage, Genes to Cells: Devoted to Molecular & Cellular Mechanisms, 10(11), 2005, pp. 1081–1091.
[6] B. Shih, D.A. McGrouther, A. Bayat, Identification of novel keloid biomarkers through profiling of tissue biopsies versus cell cultures in keloid margin specimens compared to adjacent normal skin, Eplasty 10 (2010) e24.
[7] N. Jumper, T. Hodgkinson, R. Paus, A. Bayat, Site-specific gene expression profiling as a novel strategy for unravelling keloid disease pathobiology, PLoS One 12 (3) (2017), e0172955.
[8] S. Inui, F. Shono, T. Nakajima, K. Hosokawa, S. Itami, Identification and characterization of cartilage oligomeric matrix protein as a novel pathogenic factor in keloids, Am. J. Pathol. 179 (4) (2011) 1951–1960.
[9] J. Barallobre-Barreiro, A. Didangelos, F.A. Schoendube, I. Drozdov, X. Yin, M. Fernandez-Caggiano, P. Willeit, V.O. Puntmann, G. Aldama-Lopez, A.M. Shah, N. Domenech, M. Mayr, Proteomics analysis of cardiac extracellular matrix remodeling in a porcine model of ischemia/reperfusion injury, Circulation 125 (6) (2012) 789–802.
[10] J. Barallobre-Barreiro, F. Baig, M. Fava, X. Yin, M. Mayr, Glycoproteomics of the extracellular matrix: a method for intact glycopeptide analysis using mass spectrometry, J. Vis. Exp. (122) (2017).
[11] M. van der Rest, R. Garrone, Collagen family of proteins, FASEB J. 5 (13) (1991) 2814–2823.
[12] D. Massoudi, F. Malecaze, V. Soler, J. Butterworth, A. Erraud, P. Fournie, M. Koch, S.D. Galiacy, NC1 long and NC3 short splice variants of type XII collagen are overexpressed during corneal scarring, Invest. Ophthalmol. Vis. Sci. 53 (11) (2012) 7246–7256.
[13] A. Akagi, S. Tajima, A. Ishibashi, N. Yamaguchi, Y. Nagai, Expression of type XVI collagen in human skin fibroblasts: enhanced expression in fibrotic skin diseases, J Invest Dermatol 113 (2) (1999) 246–250.
[14] S. Ricard-Blum, G. Baffet, N. Theret, Molecular and tissue alterations of collagens in fibrosis, Matrix Biol. 68-69 (2018) 122–149.
[15] J. Halper, Proteoglycans and diseases of soft tissues, Adv. Exp. Med. Biol. 802 (2014) 49–58.
[16] C.T. Ong, Y.T. Khoo, A. Mukhopadhyay, J. Masilamani, D.V. Do, I.J. Lim, T.T. Phan, Comparative proteomic analysis between normal skin and keloid scar, Br. J. Dermatol. 162 (6) (2010) 1302–1315.
[17] E. Brandan, J. Gutierrez, Role of proteoglycans in the regulation of the skeletal muscle fibrotic response, FEBS J. 280 (17) (2013) 4109–4117.
[18] L. Ala-Kokko, A. Rintala, E.R. Savolainen, Collagen gene expression in keloids: analysis of collagen metabolism and type I, III, IV, and V procollagen mRNAs in keloid tissue and keloid fibroblast cultures, J Invest Dermatol 89 (3) (1987) 238–244.
[19] J.N. Clore, I.K. Cohen, R.F. Diegelmann, Quantitative assay of types I and III collagen synthesized by keloid biopsyes and fibroblasts, Biochim. Biophys. Acta 586 (2) (1979) 384–390.
[20] D.W. Friedman, C.D. Boyd, J.W. Mackenzie, P. Norton, R.M. Olson, S.B. Deak, Regulation of collagen gene expression in keloids and hypertrophic scars, J. Surg. Res. 55 (2) (1993) 214–222.
[21] M. Trojanowska, E.C. LeRoy, B. Eckes, T. Krieg, Pathogenesis of fibrosis: type 1 collagen and the skin, J Mol Med (Berl) 76 (3–4) (1998) 266–274.
[22] J.N. Clore, I.K. Cohen, R.F. Diegelmann, Quantitation of collagen types I and III during wound healing in rat skin, Proc. Soc. Exp. Biol. Med. 161 (3) (1979) 337–340.
[23] J.C. Sible, E. Eriksson, S.P. Smith, N. Smith, Fibronectin gene expression differs in normal and abnormal human wound healing, Wound Repair Regen. 2 (1) (1994) 3–19.
[24] B. Shih, A. Bayat, Genetics of keloid scarring, Arch. Dermatol. Res. 302 (5) (2010) 319–339.
[25] S. Chung, M. Nakashima, H. Zembutsu, Y. Nakamura, Possible involvement of NEDD4 in keloid formation; its critical role in fibroblast proliferation and collagen production, Proc Jpn Acad Ser B Phys Biol Sci 87 (8) (2011) 563–573.
[26] G.K. Koukoulis, J. Shen, I. Virtanen, V.E. Gould, Vitronectin in the cirrhotic liver: an immunomarker of mature fibrosis, Hum. Pathol. 32 (12) (2001) 1356–1362.
[27] A.J. Courey, J.C. Horowitz, K.K. Kim, T.J. Koh, M.L. Novak, N. Subbotina, M. Warnock, B. Xue, A.K. Cunningham, Y. Lin, M.P. Goldklang, R.H. Simon, D.A. Lawrence, T.H. Sisson, The vitronectin-binding function of PAI-1 exacerbates lung fibrosis in mice, Blood 118 (8) (2011) 2313–2321.
[28] M.J. Randles, M.J. Humphries, R. Lennon, Proteomic definitions of basement membrane composition in health and disease, Matrix Biol. 57-58 (2017) 12–28.
[29] M. Hellstrom, S. Hellstrom, A. Engstrom-Laurent, U. Bertheim, The structure of the basement membrane zone differs between keloids, hypertrophic scars and normal skin: a possible background to an impaired function, J. Plast. Reconstr. Aesthet. Surg. 67 (11) (2014) 1564–1572.
[30] C.W. Kischer, M.R. Shetlar, M. Chvapil, Hypertrophic scars and keloids: a review and new concept concerning their origin, Scan Electron Microsc (Pt 4) (1982) 1699–1713.
[31] N. Kurokawa, K. Ueda, M. Tsuji, Study of microvascular structure in keloid and hypertrophic scars: density of microvessels and the efficacy of three-dimensional vascular imaging, J Plast Surg Hand Surg 44 (6) (2010) 272–277.
[32] P.D. Butler, Z. Wang, D.P. Ly, M.T. Longaker, A.C. Koong, G. P. Yang, Unfolded protein response regulation in keloid cells, J. Surg. Res. 167 (1) (2011) 151–157.
[33] S.L. Ashley, M. Xia, S. Murray, D.N. O'Dwyer, E. Grant, E.S. White, K.R. Flaherty, F.J. Martinez, B.B. Moore, SixSOMAmer index relating to immune, protease and angiogenic functions predicts progression in IPF, PLoS One 11 (8) (2016), e0159878.
[34] A. Menou, J. Duitman, B. Crestani, The impaired proteases and anti-proteases balance in idiopathic pulmonary fibrosis, Matrix Biol. 68-69 (2018) 382–403.
[35] M. Fonovic, B. Turk, Cysteine cathepsins and extracellular matrix degradation, Biochim. Biophys. Acta 1840 (8) (2014) 2560–2570.
[36] S. Gupta, R.K. Singh, S. Dastidar, A. Ray, Cysteine cathepsin S as an immunomodulatory target: present and future trends, Expert Opin. Ther. Targets 12 (3) (2008) 291–299.
[37] V. Turk, V. Stoka, O. Vasiljeva, M. Renko, T. Sun, B. Turk, D. Turk, Cysteine cathepsins: from structure, function and

regulation to new frontiers, Biochim. Biophys. Acta 1824 (1) (2012) 68–88.
[38] N.B. Krull, A.M. Gressner, Differential expression of keratan sulphate proteoglycans fibromodulin, lumican and aggrecan in normal and fibrotic rat liver, FEBS Lett. 312 (1) (1992) 47–52.
[39] P. Agarwal, J.N. Schulz, K. Blumbach, K. Andreasson, D. Heinegard, M. Paulsson, C. Mauch, S.A. Eming, B. Eckes, T. Krieg, Enhanced deposition of cartilage oligomeric matrix protein is a common feature in fibrotic skin pathologies, Matrix Biol. 32 (6) (2013) 325–331.
[40] R.A. Maskari Yasmin, C.M. McEniery, S.E. Cleary, Y. Li, K. Siew, N.L. Figg, A.W. Khir, J.R. Cockcroft, I.B. Wilkinson, K. M. O'Shaughnessy, The matrix proteins aggrecan and fibulin-1 play a key role in determining aortic stiffness, Sci. Rep. 8 (1) (2018) 8550.
[41] H. Outani, M. Okada, A. Yamashita, K. Nakagawa, H. Yoshikawa, N. Tsumaki, Direct induction of chondrogenic cells from human dermal fibroblast culture by defined factors, PLoS One 8 (10) (2013), e77365.
[42] L. Danisovic, I. Varga, S. Polak, Growth factors and chondrogenic differentiation of mesenchymal stem cells, Tissue Cell 44 (2) (2012) 69–73.
[43] J.H. Moon, S.S. Kwak, G. Park, H.Y. Jung, B.S. Yoon, J. Park, K.S. Ryu, S.C. Choi, I. Maeng, B. Kim, E.K. Jun, S. Kim, A. Kim, S. Oh, H. Kim, K.D. Kim, S. You, Isolation and characterization of multipotent human keloid-derived mesenchymal-like stem cells, Stem Cells Dev. 17 (4) (2008) 713–724.
[44] J. Marttala, J.P. Andrews, J. Rosenbloom, J. Uitto, Keloids: animal models and pathologic equivalents to study tissue fibrosis, Matrix Biol. 51 (2016) 47–54.
[45] C.K. Hsu, H.H. Lin, H.I. Harn, R. Ogawa, Y.K. Wang, Y.T. Ho, W.R. Chen, Y.C. Lee, J.Y. Lee, S.J. Shieh, C.M. Cheng, J.A. McGrath, M.J. Tang, Caveolin-1 controls hyperresponsiveness to mechanical stimuli and fibrogenesis-associated RUNX2 activation in keloid fibroblasts, J Invest Dermatol 138 (1) (2018) 208–218.
[46] J. Fuentes-Duculan, K.M. Bonifacio, M. Suarez-Farinas, N. Kunjravia, S. Garcet, T. Cruz, C.Q.F. Wang, H. Xu, P. Gilleadeau, M. Sullivan-Whalen, M.H. Tirgan, J.G. Krueger, Aberrant connective tissue differentiation towards cartilage and bone underlies human keloids in African Americans, Exp. Dermatol. 26 (8) (2017) 721–727.
[47] C.F. Liu, W.E. Samsa, G. Zhou, V. Lefebvre, Transcriptional control of chondrocyte specification and differentiation, Semin. Cell Dev. Biol. 62 (2017) 34–49.
[48] J. Barallobre-Barreiro, R. Oklu, M. Lynch, M. Fava, F. Baig, X. Yin, T. Barwari, D.N. Potier, H. Albadawi, M. Jahangiri, K.E. Porter, M.T. Watkins, S. Misra, J. Stoughton, M. Mayr, Extracellular matrix remodelling in response to venous hypertension: proteomics of human varicose veins, Cardiovasc. Res. 110 (3) (2016) 419–430.